



Thermoeconomic and exergoenvironmental assessments of a combined micro-gas turbine and superheated Kalina cycles for cogeneration of heat and electrical power using biomass

Z. Liu¹ · M. A. Ehyaei²

Received: 14 December 2021 / Revised: 20 March 2022 / Accepted: 1 June 2022 / Published online: 29 June 2022

© The Author(s) under exclusive licence to Iranian Society of Environmentalists (IRSEN) and Science and Research Branch, Islamic Azad University 2022

Abstract

Because non-renewable is energy resource depletion and environmental pollution, researchers and governmental policymakers considered two options: (1) replacing the non-renewable energy resource with renewable ones and (2) improving the performance of non-renewable fueled systems by considering techniques such as combined heat and power by recovering the energy of exhaust hot gas for heating utilization. In this paper, the integration of biomass-fueled micro-gas turbine (MGT) with superheated Kalina cycle was evaluated by the energy, exergy, economic and exergoenvironmental (4E) analyses. The products of this system are electrical energy produced by the superheated Kalina cycle (SKC) and MGT, as well as heating energy recovered from the gasifier. Also, other biomass types are examined and the performance of the system is investigated by using them. From the energy and exergy point of view, integration of the SKC to MGT biomass-fueled improves the system energy and exergy efficiency from 30.7% and 26.1% to 51.7% and 50.8%, respectively. In this system, the highest and lowest percentage of exergy destruction rate is related to the SKC and gasifier. The economic analysis shows this integration is beneficial and it reduces the system payback period (PP) from 9.07 to 4.6 years. The parametric study shows that increasing the air content in the gasifier improves the system performance while increasing the water content decreases it.

Keywords Micro-gas turbine · Exergy · Exergoenvironmental · Energy · Economic · Superheated Kalina cycle

Abbreviations

BC	Booster compressor
C	Compressor
CC	Combustion chamber
CHP	Combined heat and power
CPC	Combined power and cooling
Cond	Condenser
G	Generator
GT	Gas turbine
HX	Heat exchanger
ICE	Internal combustion engine
KC	Kalina cycle
MGT	Micro-gas turbine

ORC	Organic Rankine cycle
P	Pump
SKC	Superheated Kalina cycle

Greek Symbols

β	Factor
η	Efficiency
θ_{ei}	Environmental damage effectiveness index

Subscripts

0	Zero state
BC	Booster compressor
C	Compressor
CC	Combustion chamber
chi	Chemical
con	Condenser
en	Energy
ex	Exergy
fg	Vaporization
g	Gas
GT	Gas turbine
i	Inlet
i	Component number

Editorial responsibility: R Saravanan.

✉ M. A. Ehyaei
aliehyaei@yahoo.com

¹ Inner Mongolia Metallurgical Technicians College, Baotou 014010, Inner Mongolia, China

² Department of Mechanical Engineering, Pardis Branch, Islamic Azad University, Pardis new City, Iran



P	Pump
SH	Superheater
T	Turbine
tot	Total
A	Area (m ²)
C ₀	Total investment cost at reference year (\$)
C _n	Total investment cost at n year (\$)
C	Cost (\$)
CF	Annual income cash flow (\$/year)
C _p	Constant pressure Specific heat (kJ/kg.K)
e	Specific exergy (kJ/kg)
EDR	Exergy destruction rate (kW)
f _{ei}	Exergoenvironment factor
f _{es}	Exergy stability index
g	Gravitational acceleration (m/s ²)
G	Gibbs function (kJ/kg)
h	Specific enthalpy (kJ/kg)
i	Inflation rate (%)
IRR	Internal rate of return
k	Specific cost of products (\$/kWh)
K	Equilibrium constant
LHV	Lower heating value (kJ/kg)
<i>m</i>	Mass flow rate (kg/s)
n	Number of moles or years
N	Project lifetime
NPV	Net present value (\$)
P	Pressure (kPa)
PP	Payback period (years)
\dot{Q}	Heat transfer rate (kW)
r	Discount factor (%)
R	Gas constant (kJ/kgK)
r _a	Air/fuel ratio
R _u	Universal gas constant (kJ/kmoleK)
s	Specific entropy (kJ/kg.K)
SPP	Simple payback period (years)
T	Temperature (K)
V	Velocity (m/s)
\dot{W}	Power (kW)
x	Mass fraction
X	Ammonia mass fraction
y	Mole fraction
Y	Capacity of energy production in one year (kWh/year)
Z	Height (m)

Introduction

Energy demand and consumption are increased due to an increase in population and economic growth. Also, the non-renewable energy resource is limited, and it harms the

environment. The environmental issue is the main concern for every government in non-developed and developed countries (Atabi et al. 2014; Abanades et al. 2021).

To solve this problem, the usage of renewable energy resources is considered by many countries. Among this type of energy, biomass plays an important role due to availability and sustainability in any region of the world (Ahmadi et al. 2020; Cao et al. 2022). Due to various types of biomass regions, the local usage of biomass is widely spread (Situmorang et al. 2019; Abanades et al. 2022). This utilization can be divided into many categories such as heating (Herbes et al. 2018), electrical power production (Scarlat et al. 2018), upgrading to biomethane (Ryckebosch et al. 2011), transportation (Faaij 2006), and hydrogen production (Armor 1999). Electrical power generation from biogas resources is a relatively new technology in the world while it is more common in developed countries. This new technology includes gas turbine (GT) (Mohammadpour et al. 2021), internal combustion engine (ICE) (Nindhia et al. 2021), micro-gas turbine (MGT) (Sung et al. 2017), fuel cell (Hosseini 2020; Ding et al. 2019). Also, these systems can be used as combined heat and power (CHP) (Damyanova and Beschkov 2020), combined cooling and power (CPC) (Gholizadeh et al. 2019), and cogeneration (Movahed and Avami 2020) systems by utilizing the heat energy from the hot exhaust gas of the system (Quaschnig 2019). Among these mentioned technologies, an MGT is an attractive option due to lower NO_x emissions and flexibility to meet different load needs. Microturbines' size ranges are from 70 kW to over 250 kW (Mozafari et al. 2010). They can be used for different applications, especially dispersed power generation (DPG) systems to meet loads of the residential, commercial, and office buildings (Ehyaie and Bahadori 2007). Also, they have the flexibility to produce heat and cooling energies in the CHP (Ehyaie and Mozafari 2010) and CHPC states (Scarlat et al. 2018).

The application of biogas for MGT has been investigated in many research studies (Goulding and Power 2013). Renzi et al. (Renzi et al. 2017) examined the performance of a 100 kW MGT powered by syngas derived from biomass. It was shown that the overall efficiency of the MGT powered by the syngas was 27.2%, while this efficiency for natural gas was 28.6%. Furthermore, it was concluded that using the steam injection system increased electric power production, since, by variation of the injected steam from 0 to 58 g/s, the output electrical power generation changed from 100 to 129 kW. Kim et al. (Kim et al. 2017) investigated the utilization of a biogas fuel on an MGT incorporated with an organic Rankine cycle (ORC). They presented that the



MGT produced 7.4MWh heat and electrical energy annually while in combination with ORC the 8.5 MWh electrical energy was produced. In a similar study, Hosseini et al. (Hosseini et al. 2016) investigated energy and exergy analyses for a system that included an ORC and MGT powered by biogas. The electrical output power of this hybrid system was 1.4 MW while 1 MW electrical power was produced by GT and the rest of 0.4 MW was generated by the ORC cycle. The results of this study showed by increasing the gas turbine efficiency from 76 to 88% the overall energy efficiency varied from 43 to 54%, and exergy efficiency varied from 36 to 47%, respectively. Sevinchan et al. (Sevinchan et al. 2019) did energy and exergy evaluations of a biogas-fueled multigeneration system. This system includes ORC, MGT, absorption chiller, water separation unit, and recovery boiler. The results indicated that the system energy and exergy efficiencies are 72.5% and 30.4%, respectively. Bo et al. (Bo et al. 2019) investigated the energy and exergy analyses of three different configurations MGT, and ORC for electrical production, MGT and ejector refrigeration cycle (ERC), and MGT + ORC + ERC for electrical and cooling energy production. They showed that R600 as a working fluid was the worst choice for the combination of MGT + ORC while it was the best choice for the combination of an MGT + ORC + ERC. Bruno et al. (Bruno et al. 2009) compared 6 configurations of MGC, an absorption chiller to produce power and cooling energies in the sewage treatment plant. They selected the best scenario. Basrawi et al. (Basrawi et al. 2015) developed an economic methodology for biogas-fueled MGT unit sizing. They found that a combination of three types of MGT has the highest energy efficiency and the system net present value (NPV) ranges between 2.6 and 3.1 million \$. Basrawi et al. (Basrawi et al. 2012) investigated the combination of the biogas-fueled MGT located in the sewage treatment plant. They found that the number of units of MGT depends on the scale of the plant.

Rajaei et al. (Rajaei et al. 2017) did a feasibility study of micro-gas turbine units powered by biogas to meet the electrical, cooling, and heating energy needs of a rural building. Results showed the electricity cost produced by this system is around 0.446 US\$/kWh. Furthermore, Rasul and Sajjad (Rasul et al. 2015) examined biogas-fueled MGT to cover the energy requirements of a residential building in Australia. The combination of MGT with solid oxide fuel cells (SOFC) attracts the attention of researchers in current years. Moller and Rokni (Bang-Møller and Rokni 2010) the performance of the combination of SOFC and MGT

is better than each system that worked individually. They also found that (Bang-Møller et al. 2011) the combination of the SOFC, MGT, and gasifier energy efficiency is around 50.1% and it is higher than the combination of the SOFC, and gasifier (36.4%), and the combination of the MGT, and gasifier (28.1%). Wongchanapai et al. (Wongchanapai et al. 2013) did the energy and exergy analyses of direct biogas-fueled SOFC integrated by an MGT in CHP mode. They showed that increasing the compressor ratio, increases the electrical power but it decreases the useful heat generation. The combination of the SOFC, MGC, and ORC fueled by biogas is investigated by Karimi et al. (Karimi et al. 2020). Results of this research showed that the optimized system produced 329 kW electricity and 56 kW heat rate, respectively. Ebrahimi and Moradpoor (Ebrahimi and Moradpoor 2016) investigated a CHP system including SOFC, MGT, and ORC. They found that the system energy efficiency is higher than 65%. Kalina cycle (KC) was introduced as a power cycle to utilize the low-temperature energy source (Zhuang et al. 2021). The working fluid of this cycle is a mixture of ammonia and water. This cycle could be powered by different energy resources such as geothermal (Wei et al. 2015), solar (Mehrpooya et al. 2018), and waste heat in several industries (Zare et al. 2015). The usage of KC for heat recovery can be applied to various systems such as internal combustion (IC) engine (Mohammadkhani et al. 2019), diesel engine (Larsen et al. 2014), cement industry (Júnior et al. 2019), gas cycle (Feng et al. 2020). An exergoeconomic assessment of a superheated Kalina cycle powered by exhaust and coolant of a Diesel engine was performed by Mohammadkhani et al. (Mohammadkhani et al. 2019). The outcome of this study revealed that this cycle was able to generate 21.74 kW electrical power from the waste heat of a 98.9 kW Diesel engine. Also, the energy and exergy efficiencies of this cycle were calculated as 25.55% and 55.52%, respectively. Moreover, the cost of the generated power in the Kalina turbine was 15.52 cents/kWh. In another study, the assessment of a specific KC named as Split-cycle process of a KC based on exhaust heat recovery of a large marine engine was performed. The results of this study suggested that the KC with a split-cycle process obtained a thermal efficiency of 23.2% when using reheat compared to 20.8% for a conventional KC (Larsen et al. 2014). An integration hybrid of a supercritical carbon dioxide Brayton cycle and a KC powered by waste heat recovery of a marine engine was examined. The outcome of this study showed that the proposed system reduced the average annual fuel consumption

of marine power generation auxiliary engines 16.6% (Feng et al. 2020).

A careful assessment of the previous research reveals that the combination of the MGT and superheated Kalina cycle (SKC) has not been investigated, while the SKC has higher efficiency with the high-temperature source. In this study, an SKC is coupled with the MGT to utilize the heat from the exhaust hot gas of the MGT. This proposed system is powered by biomass. Also, the heat produced in the gasifier is utilized to meet the heat loads of the consumers. This proposed system is evaluated by 4E analyses. In summary, this research covers the following research gap:

- Proposing of the new cycle consists of the biogas powered by the MGT and SKC to improve the energy efficiency
- Energy, Exergy, Economic, exergoenvironmental analysis of this cycle

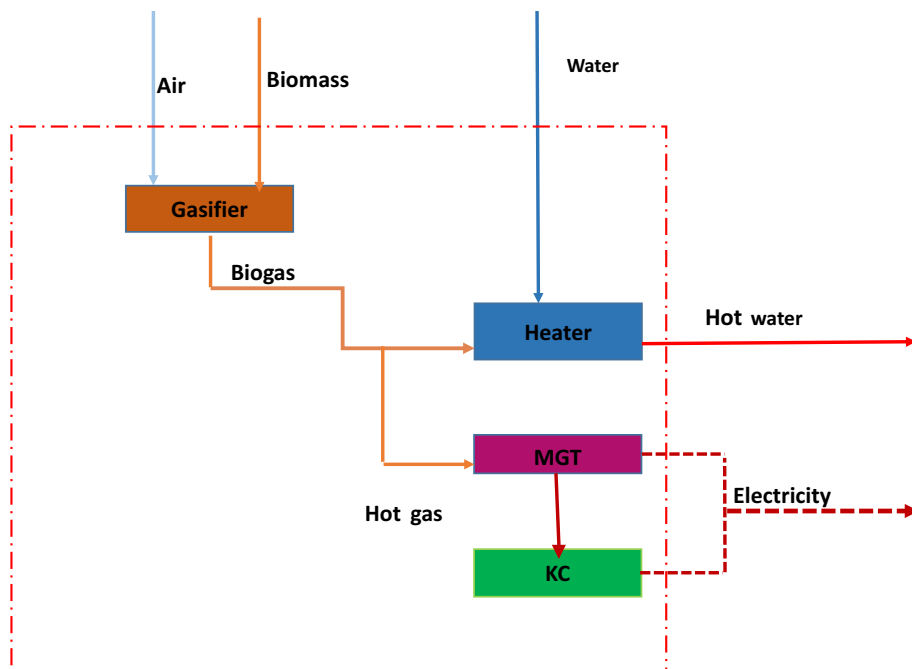
The conceptual layout of the proposed cycle is shown in Fig. 1.

Material and methods

System description

Figure 2 shows the schematic diagram of the proposed system. In this proposed system, the biomass (point 1) is reacted with air (point 2) to produce syngas (point 3) in the gasifier. The energy of the hot syngas (point 4) is utilized by water (points 21&22). Then, the syngas is pressurized with a booster compressor (BC) (point 5) and it is reacted with the air (point 7) in the combustion chamber (CC) to produce hot gas (point 8). The hot gas rotates the gas turbine (GT) and generator (G) to produce electricity (points 8&9). The heat of the exhaust hot gas is recovered in the superheater and boiler of the SKC (points 9,10,11). In the SKC, the mixture of ammonia and water is pressurized by a pump (points 20&12) and it is heated by the boiler (point 13). After the mixture goes through a separator and ammonia (point 14) and water (point 17) are separated. The ammonia superheats in the superheater (point 15) and it rotates the turbine (point 16). The water pressure (point 17) is throttled by the valve (point 18) and it is mixed with ammonia (point 19). Then,

Fig. 1 The conceptual layout of the proposed cycle



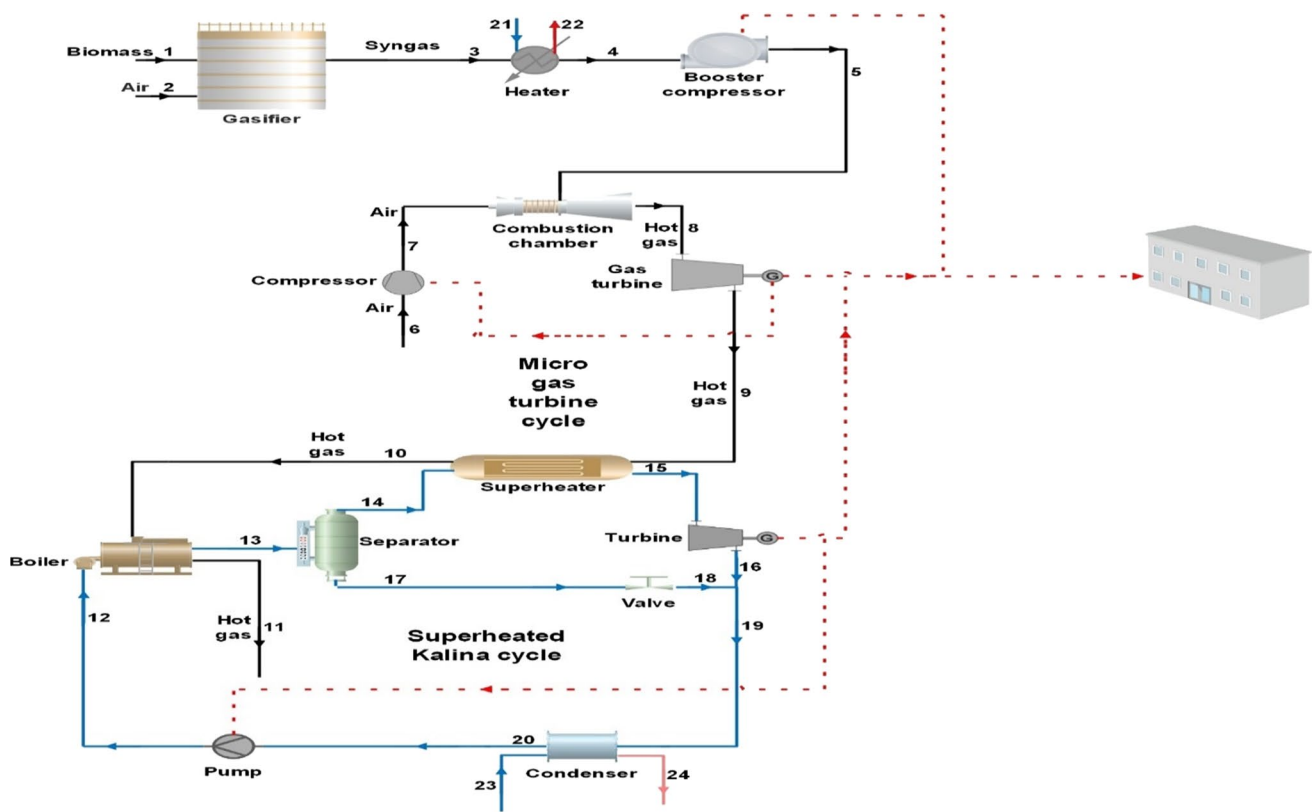


Fig. 2 The schematic diagram of the proposed system

the heat of the mixture (point 19) is transferred to the cooling water (points 20, 23, and 24). The electrical power in this proposed system is produced via turbine and GT and it is consumed via a compressor (point 6&7) and pump.

The following assumptions can be considered in this study (Mozafari et al. 2010; Ehyaei and Bahadori 2007; Ehyaei and Mozafari 2010; Karimi et al. 2020; Gholamian et al. 2018):

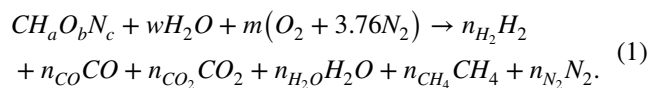
1. The system operates at the steady-state condition.
2. The heat losses in types of equipment are neglected.
3. The pressure loss in the MGT is assumed 2%.
4. The pressure loss in the SKC is ignored.
5. The ambient conditions are considered 101.103 kPa pressure and 298 K temperature.
6. The compressor and gas turbine polytropic efficiency is assumed 85% in the MGT.
7. The heat exchanger effectiveness factor is 85%.

8. The pump and turbine polytropic efficiencies in the SKC are 85%.

9. Pinch temperature is 20 K.

Energy modeling

The following reaction can be considered in the gasifier (Jarunthammachote and Dutta 2007; Soltani et al. 2013; Cao et al. 2020):



$CH_aO_bN_c$ shows the general chemical formula for biomass. The parameters a , b , c show the content of the H , O , and N in the biomass considering the elemental analysis. w depicts the moisture content. m displays the amount of the

Table 1 The MGT mass and energy balance relations for each component

No	Component	Mass balance	Energy balance
1	Compressor	$m_6 = m_7$	$\dot{W}_C = \frac{\dot{m}_6(h_2-h_1)}{\eta_c}$
2	Booster compressor	$m_4 = m_5$	$\dot{W}_{BC} = \frac{\dot{m}_4(h_5-h_4)}{\eta_{BC}}$
3	Combustion chamber	$m_5 + m_7 = m_8$	$(\dot{m}_7 h_7 + \dot{m}_8 LHV)\eta_{CC} = \dot{m}_8 h_8$
4	Gas turbine	$m_8 = m_9$	$\dot{W}_{GT} = \dot{m}_8(h_8 - h_9)\eta_{GT}$

inlet air. Considering the mass balance in Eq. 1 for the *C*, *H*, *O*, and *N* the following relation can be obtained (Jarungthammachote and Dutta 2007; Soltani et al. 2013; Karim et al. 2021):

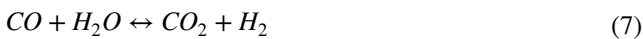
$$n_{CO} + n_{CO_2} + n_{CH_4} = 1 \tag{2}$$

$$2n_{H_2} + 2n_{H_2O} + 4n_{CH_4} = a + 2w \tag{3}$$

$$n_{CO} + 2n_{CO_2} + n_{H_2O} = b + w + 2m \tag{4}$$

$$2n_{N_2} = c + 7.52m \tag{5}$$

Also, the following equilibrium reactions are considered (Jarungthammachote and Dutta 2007; Soltani et al. 2013):



Equations 6 and 7 are related to the methane and water/gas reactions.

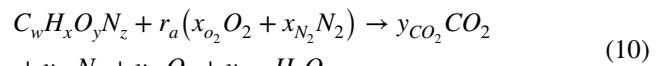
The related equilibrium constants are calculated by Jarungthammachote and Dutta (2007); Soltani et al. 2013; Noorpoor et al. 2016):

$$K = \frac{n_{CH_4} n_{tot}}{(n_{H_2})^2} \left(\frac{P_g}{P_o} \right) = \exp \left(\frac{-\Delta G}{R_u T_{gasifier}} \right) \tag{8}$$

$$K = \frac{n_{CO_2} n_{H_2}}{n_{CO} n_{H_2O}} = \exp \left(\frac{-\Delta G}{R_u T_{gasifier}} \right). \tag{9}$$

P and *T* show the pressure and temperature. ΔG shows the changes in the Gibbs free energy. *R_u* means the global gas constant. The mass and energy balance relations for the MGT are presented in Table 1.

In Table 1, *h*, *m* and η are specific enthalpy, mass flow rate, and component efficiency. The subscripts *C*, *CC*, *GT*, and *BC* are the compressor, combustion chamber, gas turbine, and booster compressor, respectively. The combustion reaction can be obtained:



$$y_{CO_2} = w \tag{11}$$

$$y_{N_2} = r_a x_{N_2} + \frac{z}{2} \tag{12}$$

$$y_{H_2O} = \frac{x}{2} \tag{13}$$

Table 2 The mass, concentration, and energy balance equations for the SKC

No	Components	Mass balance	Energy equation	X
1	Throttling value	$\dot{m}_{17} = \dot{m}_{18}$	$h_{17} = h_{18}$	$X_{17} = X_{18}$
2	Pump	$\dot{m}_{12} = \dot{m}_{20}$	$\dot{w}_p = \dot{m}_{12}(h_{12} - h_{20})$	$X_{12} = X_{20}$
4	Boiler	$\dot{m}_{10} = \dot{m}_{11}$ $\dot{m}_{12} = \dot{m}_{13}$	$\dot{m}_{10}(h_{10} - h_{11})\eta_{Boiler} = \dot{m}_{13}(h_{13} - h_{12})$	$X_{13} = X_{12}$
5	Separator	$\dot{m}_{13} = \dot{m}_{14} + \dot{m}_{17}$	$\dot{m}_{13}h_{13} = \dot{m}_{14}h_{14} + \dot{m}_{17}h_{17}$	$\dot{m}_{13}X_{13} = \dot{m}_{14}X_{14} + \dot{m}_{17}X_{17}$
6	Superheater (SH)	,	$\dot{m}_9(h_9 - h_{10})\eta_{SH} = \dot{m}_{14}(h_{15} - h_{14})$	$X_{15} = X_{14}$
7	Turbine (T)	$\dot{m}_{16} = \dot{m}_{15}$	$\dot{w}_T = \dot{m}_{15}(h_{15} - h_{16})$	$X_{16} = X_{15}$
8	Condenser	$\dot{m}_{19} = \dot{m}_{20}$	$\dot{Q}_{Con} = \dot{m}_{19}(h_{19} - h_{20}) = \dot{m}_{23}(h_{24} - h_{23})$	$X_{19} = X_{20}$

Table 3 The EDR equations for each component

No	Component	$\dot{E}_{destruction}(kW)$
1	Gasifier	$\dot{m}_1ex_1 + \dot{m}_2ex_2 - \dot{m}_3ex_3$
2	Heater	$\dot{m}_{21}ex_{21} - \dot{m}_4ex_4 + \dot{m}_3ex_3 - \dot{m}_{22}ex_{22}$
3	Booster compressor	$\dot{m}_4ex_4 - \dot{m}_5ex_5 + \dot{W}_{BC}$
4a	Compressor	$\dot{m}_5ex_5 + \dot{m}_7ex_7 - \dot{m}_8ex_8$ $\dot{m}_6ex_6 - \dot{m}_7ex_7 + \dot{W}_C$
5	Combustion chamber	
6	Gas turbine	$\dot{m}_8ex_8 - \dot{m}_9ex_9 - \dot{W}_{GT}$

Table 4 The EDR equations for the SKC

No	Components	$\dot{E}_{destruction}(kW)$
1	Pump	$\dot{m}_{20}ex_{20} - \dot{m}_{12}ex_{12} + \dot{W}_P$
2	Throttling value	$-\dot{m}_{18}ex_{18}$
3	Boiler	$\dot{m}_3ex_3 - \dot{m}_{15}ex_{15} - \dot{m}_4ex_4 + \dot{m}_{14}ex_{14}$
4	Separator	$\dot{m}_{13}ex_{13} - \dot{m}_{17}ex_{17} - \dot{m}_{14}ex_{14}$
5	Superheater (SH)	$\dot{m}_9ex_9 - \dot{m}_{15}ex_{15} - \dot{m}_{10}ex_{10} + \dot{m}_{14}ex_{14}$
6	Turbine (T)	$\dot{m}_{15}ex_{15} - \dot{W}_T - \dot{m}_{16}ex_{16}$
7	Condenser	$\dot{m}_{19}ex_{19} - \dot{m}_{24}ex_{24} - \dot{m}_{20}ex_{20} + \dot{m}_{23}ex_{23}$

$$y_{O_2} = r_a x_{O_2} + \frac{y}{2} - y_{CO_2} - \frac{y_{H_2O}}{2} \tag{14}$$

$$r_a = \frac{n_{Air}}{n_{Fuel}} \tag{15}$$

x_i and y_i present the mass and mole fractions of i . r_a depicts the air/fuel ratio.

The concentration, mass, and energy balance equations for the SKC are shown in Table 2.

Tables 2 x denotes the ammonia mass ratio. The net power production for the MGT and total system can be calculated by:

$$\dot{W}_{net,MGT} = \dot{W}_{GT} - \dot{W}_C - \dot{W}_{BC} \tag{16}$$

$$\dot{W}_{net,sys} = \dot{W}_{GT} - \dot{W}_C - \dot{W}_{BC} + \dot{W}_T - \dot{W}_P \tag{17}$$

The energy efficiency for the MGT/gasifier and the system can be obtained by:

$$\eta_{en,MGT/gasifier} = \frac{\dot{W}_{net,MGT} + \dot{m}_{22}(h_{22} - h_{21})}{\dot{m}_1LHV} \tag{18}$$

$$\eta_{en,sys} = \frac{\dot{W}_{net,sys} + \dot{m}_{22}(h_{22} - h_{21})}{\dot{m}_1LHV} \tag{19}$$

LHV means the lower heating value of biomass.

Exergy modeling

A specific exergy equation is written below (Lazzaretto and Tsatsaronis 2006; Bejan et al. 1996):

$$ex = \sum x_i ex_{chi} + \frac{V^2}{2} + gz + (h - h_0) - T_0(s - s_0) + T_0 \sum x_i R_i \ln y_i \tag{20}$$

x and ex are defined as a mass fraction and specific exergy. z , V , and g are defined as height, velocity, and gravitational acceleration. y and s denote mole fraction and entropy. Abbreviations ch , i , and 0 present as a chemical, species, and dead state condition Tables 3 and 4 show the exergy destruction rate (EDR) equations for the MGT/gasifier, and the SKC.

The exergy efficiency for the MGT/gasifier and the system can be obtained by:

$$\eta_{ex,MGT/gasifier} = \frac{\dot{W}_{net,MGT} + \dot{m}_{22}(ex_{22} - ex_{21})}{\dot{m}_1ex_1} \tag{21}$$

$$\eta_{ex,sys} = \frac{\dot{W}_{net,sys} + \dot{m}_{22}(ex_{22} - ex_{21})}{\dot{m}_1ex_1} \tag{22}$$

The biomass chemical exergy can be obtained by Kotas (2013):

$$e_{ch} = \beta(LHV + \omega h_{fg}) \tag{23}$$

$$\beta = \frac{1.0438 + 0.1882 \times (H/C) - 0.2509 \times (1 + 0.7256 \times (H/C)) + 0.0383 \times (N/C)}{1 - 0.3035 \times (N/C)} \tag{24}$$

h_{fg} denotes the enthalpy of vaporization.

Economic modeling

The proposed system annual income can be obtained by Bellos et al. (2019); Tzivanidis et al. 2016):

$$CF = Y_{elec}k_{elec} + Y_{heating}k_{heating} \tag{25}$$

k denotes products specific costs that are equal to 0.11 (Nami et al. 2018) and 0.04 (Alizadeh et al. 2020) \$/kWh for electrical and heating energy.

The system’s capital cost is calculated by Bellos et al. (2019); Tzivanidis et al. 2016; Makkeh et al. 2020):

$$C_0 = C_{MGT} + C_{SKC} + C_{gasifier} + C_{heater} \tag{26}$$

C shows the installation and investment costs. The operation and maintenance cost is assumed 3% of the initial cost (Bellos et al. 2019; Tzivanidis et al. 2016).

The effect of the inflation rate can be seen by Shafer (2017):

$$C_n = C_0(1 + i)^n \tag{27}$$

n depicts the number of years. i shows the inflation rate (3.1%) (Statista. 2021).

The simple payback period (SPP) is obtained (Bellos et al. 2019; Tzivanidis et al. 2016):

$$SPP = \frac{C_n}{CF} \tag{28}$$

The payback period (PP) is obtained by Bellos et al. (2019); Tzivanidis et al. 2016):

$$PP = \frac{\ln\left(\frac{CF}{CF-r.C_n}\right)}{\ln(1+r)} \tag{29}$$

r shows the factor of discount (3%).

The net present value (NPV) can be calculated by Bellos et al. (2019); Tzivanidis et al. 2016):

$$NPV = CF \frac{(1+r)^N - 1}{r(1+r)^N} - C_n \tag{30}$$

N presents the project lifetime (25 years).

The internal rate of return (IRR) can be obtained (Bellos et al. 2019; Tzivanidis et al. 2016; Edalati et al. 2016):

$$IRR = \frac{CF}{C_n} \left[1 - \frac{1}{(1+IRR)^N} \right] \tag{31}$$

Table 5 shows the cost function for the different components.

Exergoenvironmental assessment

To investigate the system from exergy and environmental point of views, exergoenvironmental analysis can be used (Han et al. 2020; Lv et al. 2020; Shamoushaki et al. 2021). The exergoenvironment factor can be obtained by Ratlamwala et al. (2013); Midilli and Dincer 2009; Aliehyaei et al. 2015):

$$f_{ei} = \frac{\dot{E}_{destruction}}{\sum \dot{E}x_{in}} \tag{32}$$

This factor shows the ratio of exergy destruction rate divided into the inlet exergy rate. This factor demonstrates that increasing this factor causes more exergy destruction rate that has negative effects on the environment (Ashari et al. 2012).

The environmental damage effectiveness index is expressed as (Ratlamwala et al. 2013; Midilli and Dincer 2009):

$$\theta_{ei} = f_{ei} \cdot 1/\eta_{ex} \tag{33}$$

The exergy stability index is obtained by Ratlamwala et al. (2013); Midilli and Dincer 2009):

$$f_{es} = \frac{\dot{E}_{destruction}}{\dot{E}x_{output} + \dot{E}_{destruction} + 1} \theta_{ei} = f_{ei} \cdot 1/\eta_{ex} \tag{34}$$

Table 5 The inlet design data

No	Variable	Values
1	$P_{gasifier}$	202.6 kPa
2	r_c	6.5
3	r_a	2.1
4	m (Eq. 1)	0.158
5	ω (Eq. 1)	0.34
6	\dot{m}_1	0.1 kg/s
7	T_6	298.15 K
8	T_4	358.15 K
9	T_{21}	288.15 K
10	P_{21}	101.3 kPa
12	P_{22}	101.3 kPa
13	X_{12}	0.6
14	X_{17}	0.48
15	\dot{m}_{12}	0.87 kg/s
16	\dot{m}_{14}	0.14 kg/s
17	T_{12}	298.46 K
18	P_{16}	510.8 K
19	P_{12}	2937.7 kPa
20	T_{13}	377.4 K
21	T_{16}	340.9 K

Table 6 The cost function for different components

No	Component	Cost function (\$)	Refs.
MGT			
1	Compressor	$\frac{44.71\dot{m}_6}{0.95-\eta_c} \left(\frac{P_7}{P_6}\right) \ln\left(\frac{P_7}{P_6}\right)$	Bejan et al. 1995)
2	Booster compressor	$\frac{44.71\dot{m}_4}{0.95-\eta_{BC}} \left(\frac{P_5}{P_4}\right) \ln\left(\frac{P_5}{P_4}\right)$	Khanmohammadi et al. 2015)
3	Combustion chamber	$\frac{28.98\dot{m}_7}{0.995-\frac{P_8}{P_7}} (1 + \exp(0.015(T_8 - 1540)))$	Bejan et al. 1995)
4	Gas turbine	$\left(\frac{301.45\dot{m}_8}{0.94-\eta_{GT}}\right) \ln\left(\frac{P_8}{P_9}\right) (1 + 0.025(T_8 - 1570))$	Calise and Dentice d' Accadia M et al.. 2006)
Gasifier			
5	Gasifier	$1600(3600\dot{m}_1)^{0.67}$	Khanmohammadi et al. 2015)
6	Heater	$8500 + 409A^{0.85}$	Karimi et al. 2020)
SKC			
7	Pump	$1120\dot{W}^{0.8}$	Mosaffa et al. 2017)
8	Separator	$280.3\dot{m}_{in}$	Mosaffa et al. 2017)
9	Boiler	$283\dot{Q}_{in}$	Mosaffa et al. 2017)
10	Superheater	$2143A^{0.514}$	Mosaffa et al. 2017)
11	Condenser	$2143A^{0.514}$	Mosaffa et al. 2017)
12	Turbine	$4405\dot{W}^{0.7}$	Zare et al. 2015)

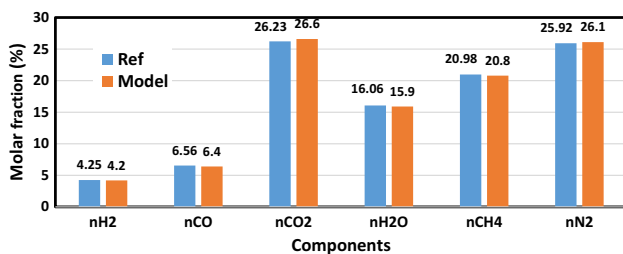


Fig. 3 The result of comparison between the data presented in the ref and the computer model for the gasifier products

Table 7 The SKC results comparison of the present research and reference (Wang et al. 2019)

Parameters	\dot{W}_p (kW)	\dot{W}_T (kW)	\dot{W}_{net} (kW)	η_{en} (%)
Ref. (Wang et al. 2019)	24.94	409.28	384.34	6.5
Model	25.3	411.3	386	6.53
Error (%)	1.44	0.49	0.43	0.46

Results and discussion

In this section, the results of the energy, exergy, economic, and exergoenvironmental analyses are presented. The biomass type is bean straw and its chemical formula can be shown as $CH_{1.5611}O_{0.7842}N_{0.0166}$ (Kanagarajan 2015). For the

mathematical modeling purpose, one computer program is written in the engineering equation solver (EES). For consideration of the thermodynamic properties, the functions that existed in the EES are used. The initial design data are presented in Table 5 (Mozafari et al. 2010; Gholamian and Zare 2016).

Model validation

Since the proposed system is novel, the validation of the whole system is not achievable. So, all of the subsystems are validated individually. For validation of the gasifier, Ref. (Kanagarajan 2015) is considered. Table 6. 3 of that reference is noticed, the biomass is considered as a bean straw. The biomass feed is 0.1294 kg/s and the intake air molar is equal to 0.0006 kmole/kmole biomass. Figure 3 shows the result of comparison between the data presented in Ref. (Kanagarajan 2015) and the output data of the computer model developed for the research. The root mean square error (RMSE) is around 3.4%.

For validation of the micro-gas turbine model, Ref. (Mozafari et al. 2010) is noticed. The inlet information presented in Table 2 of that reference is noticed. The electrical power production by the MGT in Ref. (Mozafari et al. 2010) is 29.9 kW. This value is calculated by the computer program around 29.05 kW. The error is around 2.8%. The SKC is validated by Ref. (Wang et al. 2019). The inlet data

Table 8 The thermodynamic properties at every point of the cycle

No	\dot{m} (kg/s)	P (kPa)	T (K)	h (kJ/kg)	X (-)	ex (kJ/kg)
1	0.1	101.3	298	485.7	0	21,428
2	0.08178	101.3	298	577.1	0	399.5
3	0.1818	202.6	1085	1901	0	6341
4	0.1818	172.6	358.2	627.2	0	5630
5	0.1818	658.5	545.1	954.7	0	5872
6	0.6953	101.3	298.2	577.2	0	399.5
7	0.6953	658.5	598.8	901.9	0	663
8	0.8771	638.5	1471	2020	0	1566
9	0.8771	106.4	1079	1482	0	1000
10	0.8771	104.3	762.1	953.6	0	705.6
11	0.8771	102.2	282.9	317.2	0	451.5
12	0.87	2937.7	298.5	-111.4	0.6	-94.73
13	0.87	2937.7	377.4	402.4	0.6	-22.61
14	0.14	2937.7	377.4	1430	1	230.8
15	0.14	2937.7	1059	3654	1	1490
16	0.14	510.86	340.9	1428	1	-2.455
17	0.73	2937.7	370.5	205.2	0.48	-71.48
18	0.73	510.86	329	205.2	0.48	-87.06
19	0.87	510.86	323.4	402	0.6	-75.67
20	0.87	510.86	298.5	-113.4	0.6	-97.77
21	1.77	101.3	288.2	3050	0	-9.377
22	1.77	101.3	343.2	3161	0	45.5
23	10.48	101.3	288.2	3050	0	-9.377
24	10.48	101.3	313.2	3100	0	14.81

Fig. 4 The annual electrical and heating energy produced by the MGT, gasifier, and total system

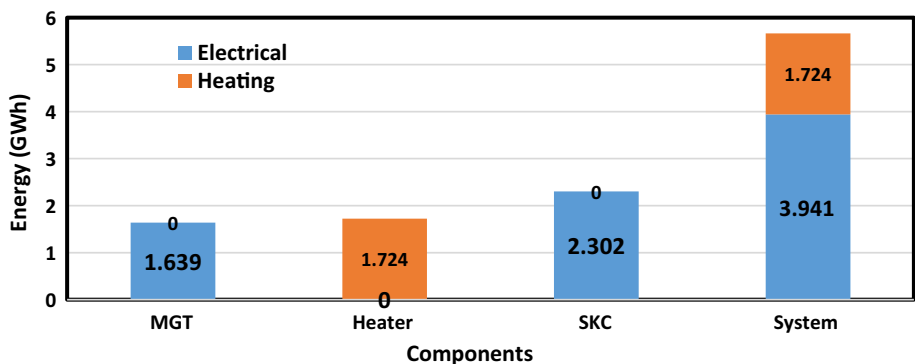


Fig. 5 The MGT + gasifier, and system energy and exergy efficiencies

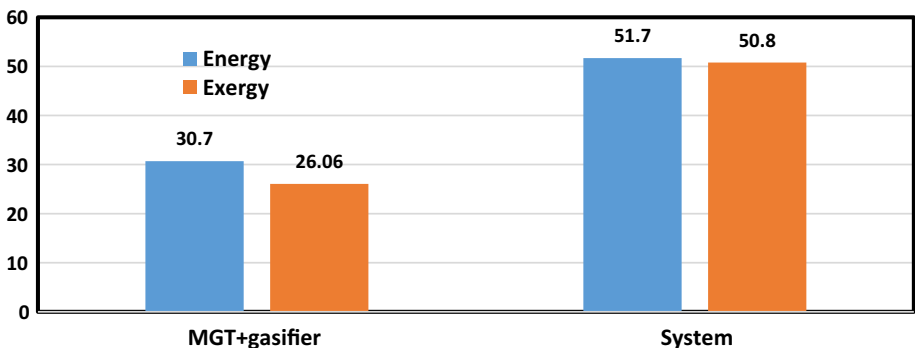


Fig. 6 The percent of the EDR in the gasifier line, MGT, SKC, and the total system

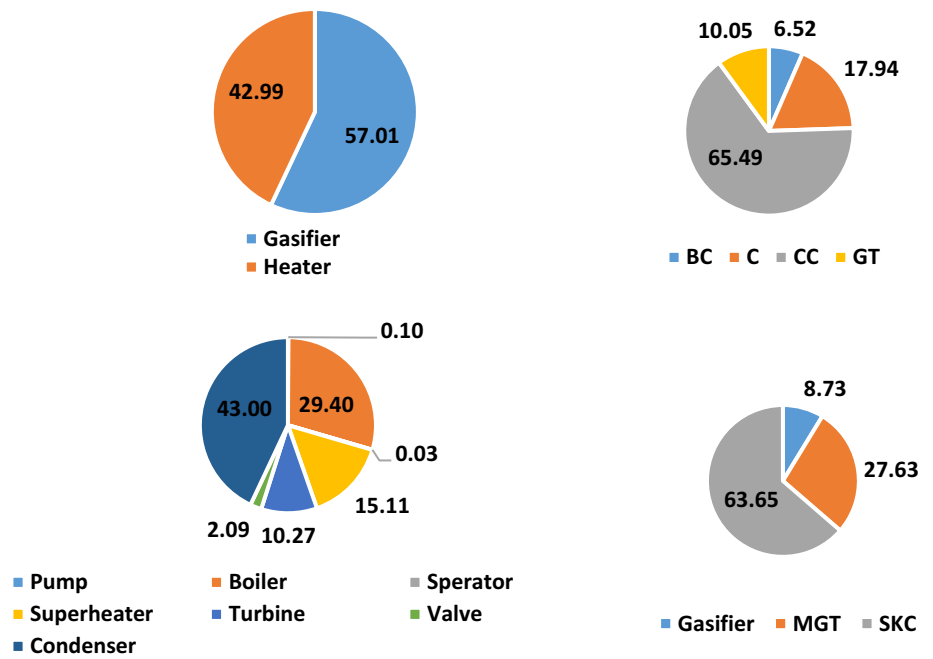


Table 9 The NPV, PP, SPP, and IRR for the system, and MGT + gasifier

No	Economic parameters	MGT + gasifier	System
1	NPV(Million\$)	2.179	6.04
2	PP(years)	9.071	4.615
3	SPP(years)	7.24	4.25
4	IRR(-)	0.1201	0.2341

depicted in Table 1 of this reference are considered. Table 7 presents the comparison results between the output data of the computer model and reference (Wang et al. 2019) for the SKC.

Table 10 The chemical formula, molecular weight, and LHV for different biomasses (Kanagarajan 2015; Basu 2010)

Cases	Name	Chemical Formula	Molecular weight (kg/kmole)	LHV (kJ/kg)
1	Oats strand	$CH_{1.269}O_{0.626}N_{0.013}$	23.46	1,2480
2	Rapeseed	$CH_{1.491}O_{0.832}N_{0.011}$	24.95	1308.4
3	Wheat straw	$CH_{1.434}O_{0.675}N_{0.031}$	24.69	13,215.2
4	Alfalfa	$CH_{1.324}O_{0.594}N_{0.063}$	23.68	12,233.8

Fig. 7 The exergoenvironmental factors (f_{ei} , θ_{ei} , f_{es}) for the MGT + gasifier and system

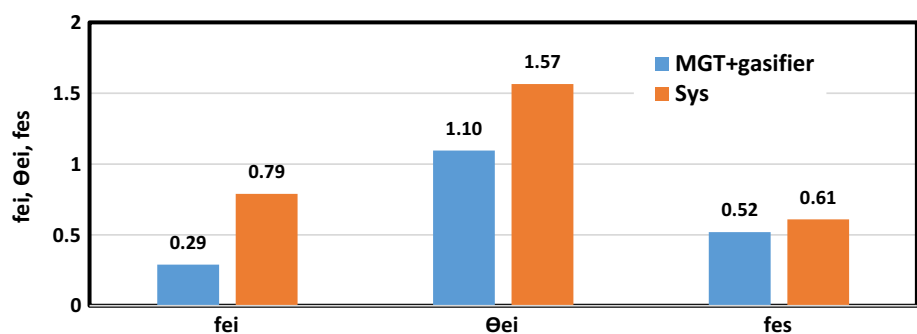


Fig. 8 The MGT + gasifier, and system energy and exergy efficiencies for various biomasses

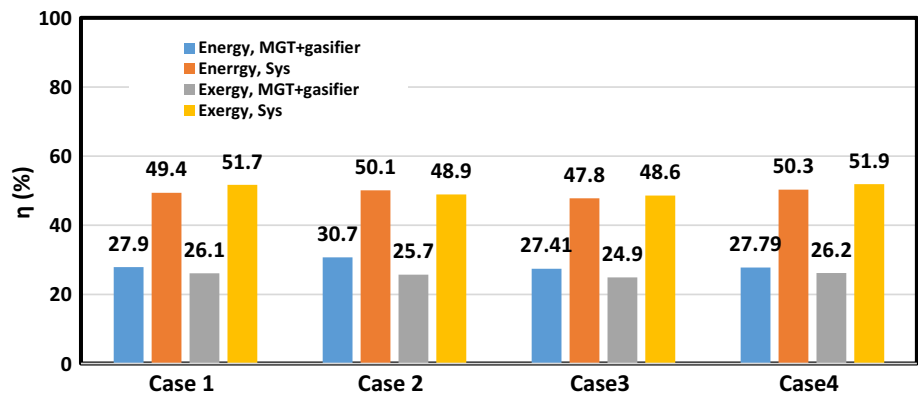
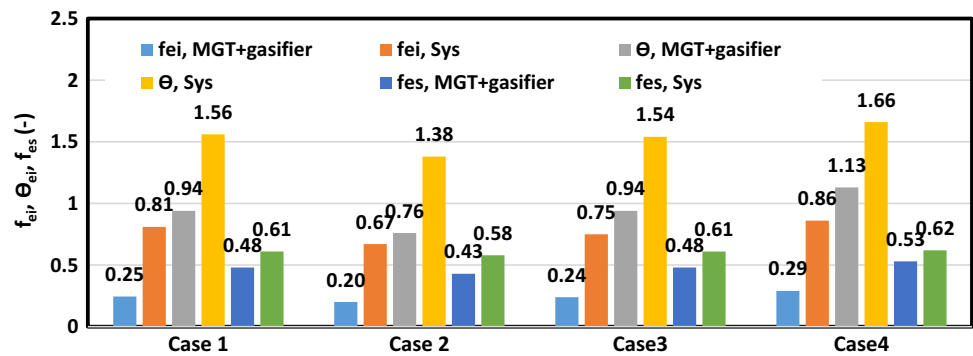


Fig. 9 The MGT + gasifier and system exergoenvironmental factors (f_{ei} , θ_{ei} , f_{es}) for various biomasses



Energy and exergy assessment

Table 8 presents the thermodynamic properties at every point of the cycle. Figure 4 depicts the annual electrical energy and heat produced by the MGT, gasifier, and the system. The MGT produces 1.639 GWh of electrical energy annually. The heater in the line of the gasifier produces 1.724 GWh of heating energy. The 2.302 GWh of electrical energy is produced by the SKC through a year if it is added to the MGT. From Fig. 4, it can be understood that adding the SKC to the MGT increased the electrical power production by around 140%. The ratio of heat to electrical energy for the total system is 43.7%.

The MGT and system energy and exergy efficiencies are depicted in Fig. 5. Adding the SKC to MGT fueled by biogas increases the system energy efficiency from 30.7% to 51.7%. This increase is about 69.4% which is a considerable increase. For the system exergy efficiency, a similar trend can be seen. It means that adding the SKC to the MGT increases the system exergy efficiency from 26.1% to 50.8%. This increase is about 93.1% (nearly twice). In general, the system exergy efficiency in both cases is lower than the system energy efficiency. The concept of heat (recovered in a

heater located in the line of biogas) differs from the work and power. The exergy rate of the heat is always much lower than the electrical power exergy rate.

The percent of the EDR for each component of the system and the subsystem is depicted in Fig. 6. The first circle shows the percent of the EDR in the line of biogas for the gasifier and heater. It is obvious that 57.01% of this value is related to the gasifier and the remaining part (42.99%) is related to the heater. The high percent of the gasifier EDR is related to the chemical reaction in the gasifier that normally has a considerable amount of exergy destruction rate. The second circle shows the percent of the EDR in each component of the MGT. The highest percent of EDR is occurred in the CC due to the combustion reaction that takes place in the CC. The lowest percent of the EDR belongs to the BC due to the lowest flow rate of the biogas that goes through it. The EDR of the GT is lower than the compressor, since the GT is a power production component and this production is reduced from the GT exergy destruction rate. The third circle is related to the percent of the EDR in every component of the SKC. The high percent of the EDR is related to the components that the heat transfer takes place in them (condenser (43.0%), boiler (29.4%), and SH (15.1%)). The lowest

percent belongs to the pump (0.1%) due to the low mass flow rate of the working fluid. In comparison between cycles (fourth circle), the highest percent of the EDR is related to the SKC (63.65%) after it, the MGT and the gasifier line have 27.63% and 8.73% of the EDR, respectively.

2.3 Economic evaluation

The NPV, PP, SPP, and IRR for the system and MGT + gasifier is presented in Table 9.

Table 10 shows that adding the SKC to the MGT + gasifier improves the economic factors. This means that adding the SKC increases the initial cost but due to an increase in system electrical power production, the system's economic benefit is improved, since the cost of products overcomes the extra initial cost of the system. For example, the NPV is improved from 2.179 to 6.04 million \$. Also, the PP and SPP are decreased from 9.071 and 7.84 to 4.615 and 4.25 years, respectively. The system IRR is increased from 0.1201 to 0.2341.

Exergoenvironmental assessment

Figure 7 shows the exergoenvironmental factors (f_{ei} , θ_{ei} , f_{es}) for the MGT + gasifier and system.

Considering Fig. 7, the f_{ei} is increased from 0.29 to 0.79 by adding the SKC, since the EDR is increased by adding any components. Similar to the f_{ei} , the θ_{ei} is increased from 1.09 to 1.56 by adding the SKC. Adding the SKC increases the f_{es} from 0.52 to 0.61, since this coupled system increases the system EDR and the output exergy rate, simultaneously. But the increase in system EDR overcomes the increase in output exergy rate in this system. So, this factor is increased. From the exergoenvironmental point of view, it is suitable that the f_{ei} , θ_{ei} , and f_{es} have the lowest value. So, increasing these factors is not suitable.

Extension of the study to other biomasses

For evaluation of the other biomasses, Table 10 can be considered (Kanagarajan 2015; Basu 2010). Table 10 shows the chemical formula, molecular weight, and LHV for different biomasses.

Figure 8 shows the MGT + gasifier, and system energy and exergy efficiencies for various biomasses depicted in Table 10. Among different biomasses, case 4 (Alfalfa),

has the highest energy and exergy efficiencies for the MGT + gasifier and system. This biomass has the lowest LHV. Case 3 (wheat straw) has the lowest energy and exergy efficiencies for the MGT + gasifier and the system. Unlike case 4, this biomass has the highest LHV.

Figure 9 shows the MGT + gasifier, and system exergoenvironmental factors (f_{ei} , θ_{ei} , f_{es}) for various biomasses depicted in Table 10. The reverse trend of Fig. 8 can be seen.

Conclusion

Due to the environmental pollution and depletion of non-renewable energy resources, the utilization of renewable energy resources has been considered by researchers. Among the type of renewable energy resources, biomass has a priority due to durability, stability, and accessibility in different regions of the world. Also, improving the system performance powered by biomass is another beneficial point. One method to improve the system performance is the utilization of the exhaust hot gas produced by the system. In this paper, the integration of the MGT biomass-fueled with the SKC was investigated. The energy, exergy, economic, and exergoenvironmental assessments were done about this system and the main parameters were calculated and compared. The main results of this article are:

- This system produced 3.94 and 1.72 GWh electrical and heating energy. The ratio of heating to electrical energy was 44%.
- Adding the SKC to MGT biomass-fueled improved the system energy and exergy efficiencies from 30.7% and 26.1% to 51.7% and 50.8%, respectively.
- Exergoenvironmental analysis showed that adding the SKC to MGT + gasifier is not beneficial, since all of the exergoenvironmental factors were increased.
- Adding the SKC to the MGT + gasifier decreased the PP and SPP from 9.1 and 7.8 years to 4.6 and 4.2 years.
- The integration increased the system NPV from 2.18 to 6.04 million \$.
- In this integration, the SKC has the highest amount of exergy destruction rate.

For future research in this regard, the SKC can be placed by different cycles such as ORC or Goswami to investigate the system performance by different configurations. Also,

the combination of different renewable energy resources such as biomass plus solar energy or biomass plus geothermal energy can be examined.

Declarations

Conflict of interest The authors believe that this paper has not any conflict of interest.

References

- Abanades S, Abbaspour H, Ahmadi A, Das B, Ehyaei MA, Esmailion F, El Haj Assad M, Hajilounezhad T, Jamali DH, Hmida A, Ozgoli HA, Safari S, AlShabi M, Bani-Hani EH (2021) A critical review of biogas production and usage with legislations framework across the globe. *Int J Environ Sci Technol* 19(4):3377–3400. <https://doi.org/10.1007/s13762-021-03301-6>
- Abanades S, Abbaspour H, Ahmadi A, Das B, Ehyaei MA, Esmailion F et al (2022) A conceptual review of sustainable electrical power generation from biogas. *Energy Sci Eng* 10(2):630–655
- Ahmadi A, Esmailion F, Esmailion A, Ehyaei MA, Silveira J (2020) Benefits and limitations of waste-to-energy conversion in Iran. *Renew Energy Res Appl* 1(1):27–45
- Aliehyaei M, Atabi F, Khorshidvand M, Rosen MA (2015) Exergy, economic and environmental analysis for simple and combined heat and power IC engines. *Sustainability* 7(4):4411–4424
- Alizadeh S, Ghazanfari A, Ehyaei M, Ahmadi A, Jamali D, Nedaei N et al (2020) Investigation the integration of heliostat solar receiver to gas and combined cycles by energy, exergy, and economic point of views. *Appl Sci* 10(15):5307
- Armor JN (1999) The multiple roles for catalysis in the production of H₂. *Appl Catal A* 176(2):159–176
- Ashari GR, Ehyaei MA, Mozafari A, Atabi F, Hajidavalloo E, Shalbal S (2012) Exergy, economic, and environmental analysis of a pem fuel cell power system to meet electrical and thermal energy needs of residential buildings. *J Fuel Cell Sci Technol*. <https://doi.org/10.1115/1.4006049>
- Atabi F, Ehyaei MA, Ahmadi MH (2014). Calculation of CH₄ and CO₂ emission rate in Kahrizak landfill site with LandGEM mathematical model. In: the 4th world sustainability forum. pp. 1–17.
- Bang-Møller C, Rokni M (2010) Thermodynamic performance study of biomass gasification, solid oxide fuel cell and micro gas turbine hybrid systems. *Energy Convers Manage* 51(11):2330–2339
- Bang-Møller C, Rokni M, Elmgaard B (2011) Exergy analysis and optimization of a biomass gasification, solid oxide fuel cell and micro gas turbine hybrid system. *Energy* 36(8):4740–4752
- Basrawi MFB, Yamada T, Nakanishi K, Katsumata H (2012) Analysis of the performances of biogas-fuelled micro gas turbine cogeneration systems (MGT-CGSs) in middle- and small-scale sewage treatment plants: Comparison of performances and optimization of MGTs with various electrical power outputs. *Energy* 38(1):291–304
- Basrawi F, Ibrahim H, Yamada T (2015) Optimal unit sizing of biogas-fuelled micro gas turbine cogeneration systems in a sewage treatment plant. *Energy Procedia* 75:1052–1058
- Basu P(2010). Biomass gasification and pyrolysis: practical design and theory. Academic press.
- Bejan A, Tsatsaronis G, Moran M (1996) Thermal design and optimization. Wiley, New York
- Bejan A, Tsatsaronis G, Moran MJ (1995) Thermal design and optimization. Wiley
- Bellos E, Pavlovic S, Stefanovic V, Tzivanidis C, Nakomcic-Smaradgakis BB (2019) Parametric analysis and yearly performance of a trigeneration system driven by solar-dish collectors. *Int J Energy Res* 43(4):1534–1546
- Bo Z, Zhang K, Sun P, Lv X, Weng Y (2019) Performance analysis of cogeneration systems based on micro gas turbine (MGT), organic Rankine cycle and ejector refrigeration cycle. *Front Energy* 13(1):54–63
- Bruno JC, Ortega-López V, Coronas A (2009) Integration of absorption cooling systems into micro gas turbine trigeneration systems using biogas: case study of a sewage treatment plant. *Appl Energy* 86(6):837–847
- Calise F, d'Accadia MD, Vanoli L, von Spakovsky MR (2006) Single-level optimization of a hybrid SOFC–GT power plant. *J Power Sources* 159(2):1169–1185
- Cao Y, Nikafshan Rad H, Hamed Jamali D, Hashemian N, Ghasemi A (2020) A novel multi-objective spiral optimization algorithm for an innovative solar/biomass-based multi-generation energy system: 3E analyses, and optimization algorithms comparison. *Energy Convers Manage* 219:112961
- Cao Y, Kasaeian M, Abbaspour H, Shamoushaki M, Ehyaei MA, Abanades S (2022) Energy, exergy, and economic analyses of a novel biomass-based multigeneration system integrated with multi-effect distillation, electro dialysis, and LNG tank. *Desalination* 526:115550
- Damyanova S, Beschkov V (2020) Biogas as a source of energy and chemicals see: <https://www.intechopen.com/books/biorefinery-concepts-energy-and-products/biogas-as-a-source-of-energy-and-chemicals>. Biorefinery concepts: Intechopen
- Ding X, Lv X, Weng Y (2019) Coupling effect of operating parameters on performance of a biogas-fueled solid oxide fuel cell/gas turbine hybrid system. *Appl Energy* 254:113675
- Ebrahimi M, Moradpoor I (2016) Combined solid oxide fuel cell, micro-gas turbine and organic Rankine cycle for power generation (SOFC–MGT–ORC). *Energy Convers Manage* 116:120–133
- Edalati S, Ameri M, Iranmanesh M, Tarmahi H, Gholampour M (2016) Technical and economic assessments of grid-connected photovoltaic power plants: Iran case study. *Energy* 114:923–934
- Ehyaei MA, Bahadori MN (2007) Selection of micro turbines to meet electrical and thermal energy needs of residential buildings in Iran. *Energy Build* 39(12):1227–1234
- Ehyaei MA, Mozafari A (2010) Energy, economic and environmental (3E) analysis of a micro gas turbine employed for on-site combined heat and power production. *Energy Build* 42(2):259–264
- Faaij A (2006) Modern biomass conversion technologies. *Mitig Adapt Strat Glob Change* 11(2):343–375
- Feng Y, Du Z, Shreka M, Zhu Y, Zhou S, Zhang W (2020) Thermodynamic analysis and performance optimization of the supercritical carbon dioxide Brayton cycle combined with the Kalina cycle for waste heat recovery from a marine low-speed diesel engine. *Energy Convers Manage* 206:112483
- Gholamian E, Zare V (2016) A comparative thermodynamic investigation with environmental analysis of SOFC waste heat to power conversion employing Kalina and Organic Rankine Cycles. *Energy Convers Manage* 117:150–161

- Gholamian E, Hanafizadeh P, Habibollahzade A, Ahmadi P (2018) Evolutionary based multi-criteria optimization of an integrated energy system with SOFC, gas turbine, and hydrogen production via electrolysis. *Int J Hydrogen Energy* 43(33):16201–16214
- Gholizadeh T, Vajdi M, Rostamzadeh H (2019) Energy and exergy evaluation of a new bi-evaporator electricity/cooling cogeneration system fueled by biogas. *J Clean Prod* 233:1494–1509
- Goulding D, Power N (2013) Which is the preferable biogas utilisation technology for anaerobic digestion of agricultural crops in Ireland: biogas to CHP or biomethane as a transport fuel? *Renew Energy* 53:121–131
- Han X, Zhang D, Yan J, Zhao S, Liu J (2020) Process development of flue gas desulphurization wastewater treatment in coal-fired power plants towards zero liquid discharge: energetic, economic and environmental analyses. *J Clean Prod* 261:121144
- Herbes C, Halbherr V, Braun L (2018) Factors influencing prices for heat from biogas plants. *Appl Energy* 221:308–318
- Hosseini SE (2020) Design and analysis of renewable hydrogen production from biogas by integrating a gas turbine system and a solid oxide steam electrolyzer. *Energy Convers Manage* 211:112760
- Hosseini SE, Barzegaravval H, Wahid MA, Ganjehkaviri A, Sies MM (2016) Thermodynamic assessment of integrated biogas-based micro-power generation system. *Energy Convers Manage* 128:104–119
- Jarungthammachote S, Dutta A (2007) Thermodynamic equilibrium model and second law analysis of a downdraft waste gasifier. *Energy* 32(9):1660–1669
- Júnior EPB, Arrieta MDP, Arrieta FRP, Silva CHF (2019) Assessment of a Kalina cycle for waste heat recovery in the cement industry. *Appl Therm Eng* 147:421–437
- Kanagarajan B, (2015) Emission and energy analysis of self-sufficient biomass power plant to achieve near net zero CO₂ emission.
- Karim SHT, Tofiq TA, Shariati M, Nikafshan Rad H, Ghasemi A (2021) 4E analyses and multi-objective optimization of a solar-based combined cooling, heating, and power system for residential applications. *Energy Rep* 7:1780–1797
- Karimi MH, Chitgar N, Emadi MA, Ahmadi P, Rosen MA (2020) Performance assessment and optimization of a biomass-based solid oxide fuel cell and micro gas turbine system integrated with an organic Rankine cycle. *Int J Hydrogen Energy* 45(11):6262–6277
- Khanmohammadi S, Atashkari K, Kouhikamali R (2015) Exergoeconomic multi-objective optimization of an externally fired gas turbine integrated with a biomass gasifier. *Appl Therm Eng* 91:848–859
- Kim S, Sung T, Kim KC (2017) Thermodynamic performance analysis of a biogas-fuelled micro-gas turbine with a bottoming organic Rankine cycle for sewage sludge and food waste treatment plants. *Energies* 10(3):275
- TJ Kotas (2013) *The exergy method of thermal plant analysis. The first edition* ed Elsevier
- Larsen U, Nguyen T-V, Knudsen T, Haglind F (2014) System analysis and optimisation of a Kalina split-cycle for waste heat recovery on large marine diesel engines. *Energy* 64:484–494
- Lazzaretto A, Tsatsaronis G (2006) SPECO: a systematic and general methodology for calculating efficiencies and costs in thermal systems. *Energy* 31(8–9):1257–1289
- Lv Q, Liu H, Wang J, Liu H, Shang Y (2020) Multiscale analysis on spatiotemporal dynamics of energy consumption CO₂ emissions in China: utilizing the integrated of DMSP-OLS and NPP-VIIRS nighttime light datasets. *Sci Total Environ* 703:134394
- Makkeh SA, Ahmadi A, Esmailion F, Ehyaei MA (2020) Energy, exergy and exergoeconomic optimization of a cogeneration system integrated with parabolic trough collector-wind turbine with desalination. *J Clean Prod* 273:123122
- Mehrpooya M, Ghorbani B, Mousavi SA (2018) Integrated power generation cycle (Kalina cycle) with auxiliary heater and PCM energy storage. *Energy Convers Manage* 177:453–467
- Midilli A, Dincer I (2009) Development of some exergetic parameters for PEM fuel cells for measuring environmental impact and sustainability. *Int J Hydrogen Energy* 34(9):3858–3872
- Mohammadkhani F, Yari M, Ranjbar F (2019) A zero-dimensional model for simulation of a Diesel engine and exergoeconomic analysis of waste heat recovery from its exhaust and coolant employing a high-temperature Kalina cycle. *Energy Convers Manage* 198:111782
- Mohammadpour M, Houshfar E, Ashjaee M, Mohammadpour A (2021) Energy and exergy analysis of biogas fired regenerative gas turbine cycle with CO₂ recirculation for oxy-fuel combustion power generation. *Energy* 220:119687
- Mosaffa AH, Hasani Mokarram N, Garousi FL (2017) Thermo-economic analysis of a new combination of ammonia/water power generation cycle with GT-MHR cycle and LNG cryogenic exergy. *Appl Therm Eng* 124:1343–1353
- Movahed P, Avami A (2020) Techno-economic optimization of biogas-fueled micro gas turbine cogeneration systems in sewage treatment plant. *Energy Convers Manage* 218:112965
- Mozafari A, Ahmadi A, Ehyaei M (2010) Optimisation of micro gas turbine by exergy, economic and environmental (3E) analysis. *Int J Exergy* 7(1):1–19
- Nami H, Ertesvåg IS, Agromayor R, Riboldi L, Nord LO (2018) Gas turbine exhaust gas heat recovery by organic Rankine cycles (ORC) for offshore combined heat and power applications—Energy and exergy analysis. *Energy* 165:1060–1071
- Nindhia TGT, McDonald M, Styles D (2021) Greenhouse gas mitigation and rural electricity generation by a novel two-stroke biogas engine. *J Clean Prod* 280:124473
- Noorpoor A, Heidarnajad P, Hashemian N, Ghasemi A (2016) A thermodynamic model for exergetic performance and optimization of a solar and biomass-fuelled multigeneration system. *Energy Equip Sys* 4(2):281–289
- Quaschnig VV (2019) *Renewable energy and climate change* Wiley.
- Rajaei G, Atabi F, Ehyaei M (2017) Feasibility of using biogas in a micro turbine for supplying heating, cooling and electricity for a small rural building. *Adv Energy Res* 5(2):129–145
- Rasul MG, Ault C, Sajjad M (2015) Bio-gas mixed fuel micro gas turbine co-generation for meeting power demand in Australian remote areas. *Energy Procedia* 75:1065–1071
- Ratlamwala TA, Dincer I, Gadalla MA (2013) Comparative environmental impact and sustainability assessments of hydrogen and cooling production systems. Springer, Causes, impacts and solutions to global warming, pp 389–408
- Renzi M, Patuzzi F, Baratieri M (2017) Syngas feed of micro gas turbines with steam injection: effects on performance, combustion and pollutants formation. *Appl Energy* 206:697–707
- Ryckebosch E, Drouillon M, Vervaeren H (2011) Techniques for transformation of biogas to biomethane. *Biomass Bioenergy* 35(5):1633–1645
- Scarlat N, Dallemand J-F, Fahl F (2018) Biogas: developments and perspectives in Europe. *Renew Energy* 129:457–472
- Sevinchan E, Dincer I, Lang H (2019) Energy and exergy analyses of a biogas driven multigenerational system. *Energy* 166:715–723
- Shafer T (2017) Calculating inflation factors for cost estimates. Pregamon, City of Lincoln transportation and utilities project delivery
- Shamoushaki M, Aliehyaei M, Taghizadeh-Hesary F (2021) Energy, exergy, exergoeconomic, and exergoenvironmental assessment of flash-binary geothermal combined cooling, heating and power cycle. *Energies* 14(15):4464



- Situmorang YA, Zhao Z, Yoshida A, Kasai Y, Abudula A, Guan G (2019) Potential power generation on a small-scale separated-type biomass gasification system. *Energy* 179:19–29
- Soltani S, Mahmoudi SMS, Yari M, Rosen MA (2013) Thermodynamic analyses of a biomass integrated fired combined cycle. *Appl Therm Eng* 59(1):60–68
- Statista (2021) Global inflation rate compared to previous year See: <https://www.statista.com/statistics/256598/global-inflation-rate-compared-to-previous-year/>
- Sung T, Kim S, Kim KC (2017) Thermo-economic analysis of a biogas-fueled micro-gas turbine with a bottoming organic Rankine cycle for a sewage sludge and food waste treatment plant in the Republic of Korea. *Appl Therm Eng* 127:963–974
- Tzivaniadis C, Bellos E, Antonopoulos KA (2016) Energetic and financial investigation of a stand-alone solar-thermal organic rankine cycle power plant. *Energy Convers Manage* 126:421–433
- Wang J, Wang J, Zhao P, Dai Y (2019) Proposal and thermodynamic assessment of a new ammonia-water based combined heating and power (CHP) system. *Energy Convers Manage* 184:277–289
- Wei G, Meng J, Du X, Yang Y (2015) Performance analysis on a hot dry rock geothermal resource power generation system based on kalina cycle. *Energy Procedia* 75:937–945
- Wongchanapai S, Iwai H, Saito M, Yoshida H (2013) Performance evaluation of a direct-biogas solid oxide fuel cell-micro gas turbine (SOFC-MGT) hybrid combined heat and power (CHP) system. *J Power Sources* 223:9–17
- Zare V, Mahmoudi SMS, Yari M (2015) On the exergoeconomic assessment of employing Kalina cycle for GT-MHR waste heat utilization. *Energy Convers Manage* 90:364–374
- Zhuang Y, Zhou C, Dong Y, Du J, Shen S (2021) A hierarchical optimization and design of double Kalina cycles for waste heat recovery. *Energy* 219:119593

